

Proceeding Paper

# Advanced Quartz Microbalance Sensors for Gas-Phase Applications: Effect of Adsorbate on Shear Bond Stiffness between Physical Transducer and Superlattice of Latex Nanoparticles <sup>†</sup>

Ivanna Kruglenko <sup>\*</sup>, Sergii Kravchenko, Petro Kruglenko, Julia Burlachenko, Iryna Krishchenko , Edward Manoilov and Boris Snopok 

Department of Optoelectronics, V.E. Lashkaryov Institute of Semiconductor Physics, National Academy of Sciences of Ukraine, 41 Pr. Nauki, 03028 Kyiv, Ukraine

<sup>\*</sup> Correspondence: [kruglen@isp.kiev.ua](mailto:kruglen@isp.kiev.ua)

<sup>†</sup> Presented at the 9th International Electronic Conference on Sensors and Applications, 1–15 November 2022; Available online: <https://ecsa-9.sciforum.net>.



**Citation:** Kruglenko, I.; Kravchenko, S.; Kruglenko, P.; Burlachenko, J.; Krishchenko, I.; Manoilov, E.; Snopok, B. Advanced Quartz Microbalance Sensors for Gas-Phase Applications: Effect of Adsorbate on Shear Bond Stiffness between Physical Transducer and Superlattice of Latex Nanoparticles. *Eng. Proc.* **2022**, *27*, 40. <https://doi.org/10.3390/ecsa-9-13204>

Academic Editor: Francisco Falcone

Published: 1 November 2022

**Publisher's Note:** MDPI stays neutral with regard to jurisdictional claims in published maps and institutional affiliations.



**Copyright:** © 2022 by the authors. Licensee MDPI, Basel, Switzerland. This article is an open access article distributed under the terms and conditions of the Creative Commons Attribution (CC BY) license (<https://creativecommons.org/licenses/by/4.0/>).

**Abstract:** New sensitive architectures built on soft surface architectures or nano-sized blocks also require a rethinking of the principles of the operation of traditional physical recording methods. Here, we report an experimental study of complex loadings for classical quartz crystal microbalance (QCM) that appear on the surface with flexible spatial organization and variable coupling by which the interface architecture is connected to the transducer. Sensitive layers are superlattices formed on 100 nm LB1 latex nanoparticles self-assembled during the contact line deposition in evaporating sessile droplets with or without nonionic surfactant TWEEN<sup>®</sup> 20. It was shown that QCM resonance frequency change is not primarily determined by the adsorbate mass alone (as for LB1&TWEEN<sup>®</sup> 20 mixture), but rather by the link by which interfacial architecture is bound to the transducer (as for LB1 superlattice). A model has been proposed and substantiated in which the manifestation of anti-Sauerbrey behavior is associated with changes under the action of water vapor in the characteristics of the contact area of intra-film 3D mountainous deposits with the transducer surface. The possibility of a gaseous analyte not only to change the loading of QCM but also the features of the mechanical behavior of the mass associated with the surface opens the way to the creation of a new class of highly selective sensors of especially dangerous or critically important analytes. Due to the selective effect of the analyte on the processes of interfacial friction in the contact layer between the sensitive architecture and the sensor substrate, a contrast pattern of response to the target analyte can be formed. This is due not so much to the large magnitude of the response itself, but to the fact that the change in the analytical signal is opposite to the “usual” Sauerbray-like shift of the resonant frequency.

**Keywords:** quartz crystal microbalances; complex loadings; latex nanoparticles; nanoparticle superlattice; anti-Sauerbrey behavior; adsorption

## 1. Introduction

Quartz crystal microbalance (QCM) is one of the oldest and most predominant techniques utilizing the electro-mechanical resonance phenomena in bulk piezoelectric resonators occurring in the MHz range. Because of the small size of QCM transducers, the simplicity of their construction and operation, low weight and price, small energy consumption, high sensitivity ( $0.1\text{--}1.0\text{ Hz cm}^2\text{ ng}^{-1}$ ), stability, and broad market availability, QCM-based acoustic sensors represent a popular analytical tool for high precision analytical mass sensing with real-time capability and label-free detection principle.

Despite a number of successful applications of the Sauerbrey equation for the analysis of QCM data in analytical science, in the last decade, there have been more and more

examples of the so-called anti-Sauerbrey behavior of QCM sensors, associated with the peculiarities of the interaction of target analytes with a sensitive layer [1–5]. Instead of a decrease in the QCM response as predicted by the Sauerbrey equation, a positive resonant frequency shift was observed with the increase in the mass of the adsorbate in many publications. All of them may be interpreted within the Sauerbrey concept as processes with “negative, missing mass”, or mass deficit.

Whereas the new generation of advanced sensors is intended to use complex interfacial sensing architectures, future progress in QCM-based instrumentation will require an increased understanding of the relation between the changes in frequency and the properties of such more complex loadings. These advancements will have a tremendous impact on the correctness and effectiveness of QCM instrumentation in future applications, especially for complex sensing architectures based on nanoparticle ensembles. Such sensitive layers are obtained by various methods, including thermal spraying, the layering of polyions of different signs, LB technology, and the specific binding of proteins and polysaccharides, as well as precipitation from a solution using solvent evaporation. Recently, drying methods have become increasingly involved in obtaining thin layers of organic nanoparticles, latex spheres, and even microorganisms. This makes it possible to obtain so-called nanoparticle superlattices, which are periodic arrays of nanosized inorganic building blocks, including metal nanoparticles, quantum dots, and magnetic nanoparticles. In this paper, we will consider the behavior of quartz microbalance transducers when their surface is loaded with nanoparticle superlattices based on latex particles.

## 2. Materials and Methods

The LB1 nanoparticles of polystyrene latex beads (Sigma-Aldrich) are negative charge-stabilized colloidal particles with a mean diameter of 100–120 nm, a latex density of approximately 1.005 g/mL, and a refractive index of about 1.6 in the visible region. The negative surface charge is due to the sulfate group terminated polymer chains located on the particle surface where they interact with the aqueous phase.

Silver electrodes located on both sides of the QCM transducer were evenly coated with 20  $\mu$ L of an aqueous suspension (single drop) of LB1 latex particles or their mixture with 0.2% TWEEN<sup>®</sup> 20 surfactant (20  $\mu$ L) and dried at room temperature for 24 h.

An original multichannel QCM analyzer has been used for the investigations. The analyzer contains (i) a temperature-controlled measurement camera with the sensors matrix of the flowing type; (ii) a quartz generators block (10 MHz); (iii) a block of the frequency measurement and an RS232 sequential interface constructed on the base of specialized microprocessor (AT89C2051); (iv) a generator of the gas mixtures; (v) system collection and processing of the information on the base of a personal computer [6–8]. The system temperature was maintained at the  $21 \pm 1$  °C level, and the consumption of the carrier gas (argon) was about 180 mL/min. The measurement procedure included the next stages: gas circulation up to the frequency stabilization of the sensors ( $\pm 3$  Hz); the circulation of the vapor–gas mixture; purging by carrier gas up to the restoration of the initial frequency value of the QCM.

## 3. Results and Discussion

Nanoparticle superlattices represent a new class of materials with collective properties that differ from those of bulk-phase crystals or isolated nanocrystals. Such new structures are of considerable interest, in particular, because they can be fabricated using an extremely simple technological technique. The drying-mediated assembly is driven by both the specific and nonspecific (entropy-driven) interactions of particles under the conditions of volume reduction due to the evaporation of the solvent. For example, the evaporation of water droplets containing polystyrene (PS) particles on the surface usually results in the formation of a compact monolayer coating (for low concentrations of particles) or mountainous deposits (for high concentrations) [9]. Indeed, unlike the situation when the concentration of microparticles is low and the contact radius of a water drop decreases

throughout the entire process, the evaporation of a water drop with a higher concentration of microparticles is more difficult. The gradual packing of nanoparticles into aggregates is based on entropy effects; nanoparticles in superlattices spontaneously assemble into local structures minimizing the free energy of the system. Capillary flows induced by nonuniform evaporation fields and fluctuations in liquid composition, shape, surface tension, etc. during drying inside the droplet lead to irregular features with kinetically trapped local structures. As a result, separate three-dimensional hierarchical structures embedded in a common organic coating can be formed.

Unfortunately, the fabrication of superlattices is still a non-trivial task, since nanoparticles are difficult to manipulate due to the complex nanoscale forces among them, which also change during the formation of a solid structure. Non-ionic surfactants such as TWEEN<sup>®</sup> 20 can be used as effective agents to prevent spontaneous aggregation and increase the kinetic stability of colloidal solutions of polystyrene (PS) particles.

In this paper, we consider a series of samples created simultaneously in the framework of the scenario outlined above. Superlattices of LB1 and their mixtures with TWEEN<sup>®</sup> 20 were obtained from highly concentrated aqueous solutions on smooth (RMS roughness of several nanometers) surfaces of silver electrodes of QCM transducers and silicon wafers for additional characterization. The deposition was carried out under conditions where the number of particles in a solution drop was approximately two orders of magnitude greater than the geometric projection area of the metal electrode (the drop contained approximately  $10^{12}$  particles, while about  $10^{10}$  particles are required for a monolayer coating with 100 nm spheres of an area of an electrode 10 mm in diameter). Such conditions uniquely ensure the three-dimensional nature of the surface structure.

These changes in the frequency of QCM transducers before and after the deposition of a layer of nanoparticles indicate that for a solution of nanoparticles with TWEEN<sup>®</sup> 20, the response of the QCM is in good agreement with the estimates of the mass of particles in the solution formed on the basis of the information provided by the manufacturer. Indeed, with the latex density of approximately 1.005 g/mL, the total mass of particles deposited on both QCM electrodes is in good agreement with responses of approximately “-” 50 kHz with a typical sensitivity of about 1 ng/Hz (taking into account the Gaussian-like shape of the sensitivity profile across the electrode area). It should be noted that the variation in the load for different transducers, in this case, was insignificant and could be due to the uneven distribution of mass on the surface. When applying the nanoparticles’ film, a decrease in the frequency of the transducer is observed in full accordance with the Sauerbrey theory.

A fundamentally different behavior is observed for transducers on which an aqueous solution of highly concentrated latex nanoparticles without TWEEN<sup>®</sup> 20 was used for deposition. In this case, the measured loading of the sensors varies over a wide range from “-” 40 kHz to almost “+” 3 MHz. This behavior is typical for QCM transducers, the operation of which, for some reason, no longer corresponds to the Sauerbrey model [1]. In most cases, this behavior is due to the fact that the sensitive layer no longer has a strong mechanical contact with the surface of the transducer, and its oscillations are out of phase with the movement of the substrate. Since the responses to gaseous analytes with different loads were qualitatively similar (the responses with positive loads were characterized by unstable behavior with the presence of local frequency spikes) we will consider a transducer with a load of about “-” 40 kHz as a representative of LB1 structures.

Figure 1a shows the responses of QCM transducers modified with LB1 and LB1-TWEEN<sup>®</sup> 20 mixture when saturated ethanol vapor is blown over their surface. As can be seen from the figure, the response has a classical shape with a decrease in the resonant frequency as the adsorbate accumulates on the sensitive element. If we compare these responses with those for conventional organic coatings such as phthalocyanines, etc., then only the magnitude of the response differs—an increase in the response by about an order of magnitude is observed, which can be explained by an increase in the surface area [10–12]. The difference in the response for the LB1 and LB1&TWEEN<sup>®</sup> 20 sensitive layers is not essential since it can be caused by the adsorption properties of detergent molecules or the

structure of the film. An approximation of the response shape indicates that the process is due to adsorption on the surface and follows the Langmuir model [13,14] well. On the whole, both structures demonstrate a response following the Sauerbrey model, which suggests that the adsorption of alcohol molecules does not change the viscoelastic properties of the coating or its bond with the transducer surface.

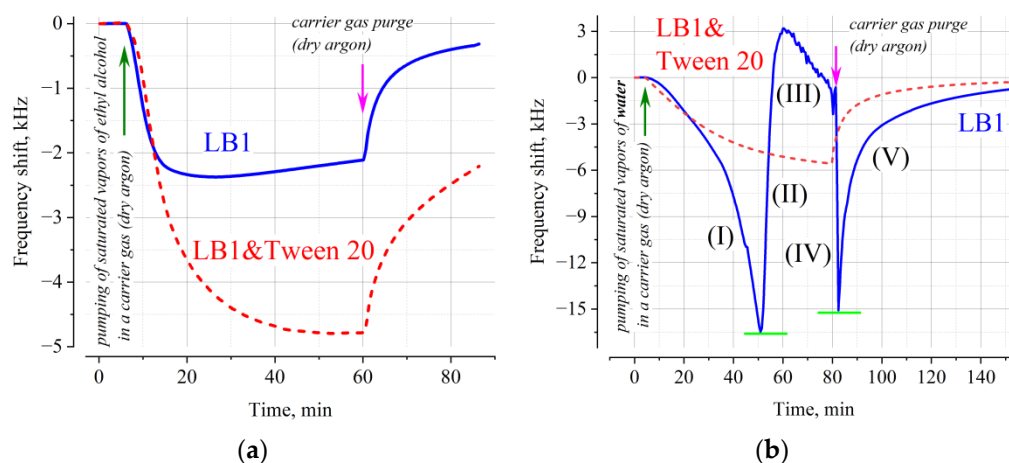


**Figure 1.** The typical responses of QCM transducers modified with LB1 and a mixture of LB1 with TWEEN<sup>®</sup> 20 when saturated ethyl alcohol (a) or water (b) vapors are pumped over their surface.

Figure 1b shows the dependences of the response of the QCM transducers modified with LB1 and an LB1&TWEEN<sup>®</sup> 20 mixture when saturated water vapor is pumped over their surface. As can be seen from the figure, the response of the sensor coated with a mixture of nanoparticles and detergent has a classical form with a decrease in the resonant frequency as the adsorbate accumulates on the sensitive element; moreover, both the shape of the dependence and the magnitude of the response are similar to those for saturated vapors of ethyl alcohol (Figure 1a). At the same time, the response of the LB1-coated sensor has a qualitatively different dependence. The initial drop in frequency (I) is replaced by its sharp increase (II) after reaching approximately “−17 kHz; the frequency increases to a value much greater than the initial reference “zero” baseline, which clearly indicates a change in the mechanical properties of the surface architecture. Then, again at stage (III), there is a slightly slower decrease in frequency compared to the initial stage (I). Purging with carrier gas initially returns the system to the state it was in at the end of the phase (I), reducing the value of frequency drastically through the process (IV). Additionally, only after that is there observed a typical desorption process (V), the reverse of process (I). This behavior unequivocally testifies in favor of the fact that there is some trigger element in the system, the operation of which, upon the adsorption of a certain amount of water, abruptly changes the mechanical characteristics of the surface architecture.

In order to clarify the possible structure of such a trigger element, similar samples were formed on the surface of a silicon wafer, photographs of which in an optical microscope are shown in Figure 2. As can be seen from the figure, in the case of the presence of nonionic surfactant in a mixture with latex nanoparticles, the microstructure represents separate solid fragments randomly located and oriented on the surface. The fragments have a fairly large area; significant differences in the optical density of their optical images are not observed. At the same time, for a film based on LB1 nanoparticles, smoother contours of the formed structures are observed, the shape of which is probably due to the front of a drying drop controlled by the surface tension gradient. Of the greatest interest are the observed round regions, the structure of which, the distribution of intensities, and the color gamut of the rings in white light indicate their interference nature. As is well known, it is precisely such annular interference maxima and minima that appear around the point of

contact of a convex lens and a plane-parallel plate when light passes or reflects through the lens (the so-called Newton's rings).

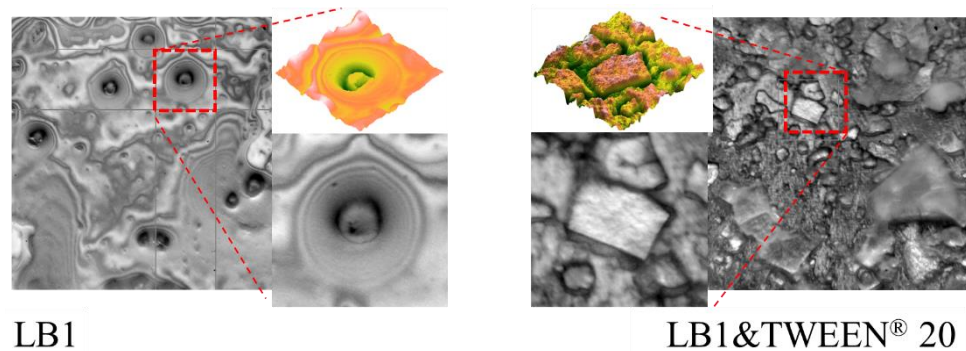


**Figure 2.** Images of surface structures based on superlattices of latex particles LB1 and their mixture with nonionic surfactant TWEEN® 20 obtained in an optical microscope. The 3D images (built using the Gwyddion software environment) of the enlarged areas are shown for illustrative purposes only to more clearly emphasize the symmetry of the optical structure of the image.

In the classical version, the cause of this phenomenon is the constructive interference and mutual damping of waves reflected from the convex surface of the lens at the glass–air interface, and a flat plate at the air–glass interface. The appearance of a similar picture in our case means that in the vicinity of such a microdefect (probably a 3D mountainous deposit of nanoparticles in the form of a “convex lens”), there are voids located near the substrate filled with a medium with a refractive index lower than that of the latex structure (probably air, in the absence of water vapor). If there are saturated water vapors in the surrounding space, they penetrate and fill these voids. Capillary forces, as well as the high surface tension of water, contribute to this process and stimulate the local disruption of the mechanical adhesion of the nanoparticle cluster to the substrate. This causes the slippage of the cluster and a change in the rigid connection of a part of the film with the substrate, and manifests itself in an increase in frequency. All the above features of the behavior of QCM with a layer of the LB1 superlattice are well explained by this model.

#### 4. Conclusions

This paper illustrates the fact that for QCM sensors, important properties of matter include not only its load but also the internal structure of the sensing architecture and its mechanical properties. Thus, in reality, QCM resonance frequency change is not primarily determined by the adsorbate mass alone, but rather by the link by which interfacial architecture is bound to the transducer. In particular, this paper shows that the “transformation” of Sauerbrey into anti-Sauerbrey behavior of QCM sensors can be associated with the formation of mechanical nonlinear contact, accompanied by a change in friction in the area of the contact area on the surface. Thus, “massive” interfacial ensembles LB1 with weak interfacial adhesion are able to slide along the substrate under the infusion of water vapor; a mechanically unbound massive cluster is able to freely move its center of mass over the surface, violating the laws of classical behavior in the Sauerbrey model. Thus, the volatile compound is able to not only change the mass load of the quartz microbalance sensor but also induce a transition to anti-Sauerbrey behavior owing to a rigidity change or interfacial friction variations under bulk phase sorption or surface adsorption. Such undocumented capabilities of QCM transducers and sensors thereon open up new possibilities for creating new approaches for forming virtual sensor arrays [15] and creating more universal protocols within electronic nose technologies [16–22].

**Author Contributions:** Conceptualization, B.S. and I.K. (Ivanna Kruglenko); methodology, B.S., I.K. (Ivanna Kruglenko), and S.K.; validation, sample preparation S.K. and I.K. (Ivanna Kruglenko); investigation, I.K. (Ivanna Kruglenko), S.K. and P.K.; writing—original draft preparation, I.K. (Ivanna Kruglenko) and B.S.; writing—review and editing, I.K. (Ivanna Kruglenko), S.K., J.B., I.K. (Iryna Krishchenko), E.M. and B.S. All authors have read and agreed to the published version of the manuscript.

**Funding:** This research received no external funding.

**Institutional Review Board Statement:** Not applicable.

**Informed Consent Statement:** Not applicable.

**Data Availability Statement:** Data are available on request.

**Conflicts of Interest:** The authors declare no conflict of interest.

## References

1. Kravchenko, S.; Snopok, B. “Vanishing mass” in the Sauerbrey world: Quartz Crystal Microbalance study of self-assembled monolayers based on tripod-branched structure with tuneable molecular flexibility. *Analyst* **2020**, *145*, 656. [[CrossRef](#)] [[PubMed](#)]
2. Hauptmann, P.; Lockley, R.; Hartmann, J.; Auge, J. Using the quartz microbalance principle for sensing mass changes and damping properties. *Sens. Actuators A* **1993**, *37–38*, 309–316. [[CrossRef](#)]
3. Liang, C.; Yuan, C.-Y.; Warmack, R.J.; Barnes, C.E.; Dai, S. Ionic Liquids: A New Class of Sensing Materials for Detection of Organic Vapors Based on the Use of a Quartz Crystal Microbalance. *Anal. Chem.* **2002**, *74*, 2172–2176. [[CrossRef](#)] [[PubMed](#)]
4. Toniolo, R.; Pizzariello, A.; Dossi, N.; Lorenzon, S.; Abollino, O.; Bontempelli, G. Room temperature ionic liquids as useful overlayers for estimating food quality from their odor analysis by quartz crystal microbalance measurements. *Anal. Chem.* **2013**, *85*, 7241–7247. [[CrossRef](#)] [[PubMed](#)]
5. Johannsmann, D.; Reviakine, I.; Rojas, E.; Gallego, M. Effect of sample heterogeneity on the interpretation of QCM(-D) data: Comparison of combined quartz crystal microbalance/atomic force microscopy measurements with finite element method modeling. *Anal. Chem.* **2008**, *80*, 8891–8899. [[CrossRef](#)] [[PubMed](#)]
6. Kruglenko, I.V.; Snopok, B.A.; Shirshov, Y.M.; Venger, E.F. Digital aroma technology for chemical sensing: Temporal chemical images of complex mixtures. *Semicond. Phys. Quantum Electron. Optoelectron.* **2000**, *3*, 529–541. [[CrossRef](#)]
7. Kruglenko, I.V.; Snopok, B.A.; Shirshov, Y.M.; Rowell, F.J. Multisensor systems for gas analysis: Optimization of the array for the classification of the pharmaceutical products. *Semicond. Phys. Quantum Electr. Optoelectron.* **2004**, *7*, 207–216. [[CrossRef](#)]
8. Snopok, B.; Kruglenko, I. Analyte induced water adsorbability in gas phase biosensors: The influence of ethinylestradiol on the water binding protein capacity. *Analyst* **2015**, *140*, 3225–3232. [[CrossRef](#)] [[PubMed](#)]
9. Yu, Y.S.; Wang, M.C.; Huang, X. Evaporative deposition of polystyrene microparticles on PDMS surface. *Sci. Rep.* **2017**, *7*, 14118. [[CrossRef](#)] [[PubMed](#)]
10. Burlachenko, Y.u.V.; Snopok, B.A.; Capone, S.; Siciliano, P. Performance of Machine Olfaction: Effect of Uniqueness of the Initial Data and Information Coding on the Discrimination Ability of Multisensor Arrays. *IEEE Sens. J.* **2011**, *11*, 649–656. [[CrossRef](#)]
11. Burlachenko, J.V.; Snopok, B.A. Multisensor arrays for gas analysis based on photosensitive organic materials: An increase in the discrimination capacity under selective illumination conditions. *J. Anal. Chem.* **2008**, *63*, 610–619. [[CrossRef](#)]
12. Snopok, B.A.; Kruglenko, I.V. Nonexponential relaxations in sensor arrays: Forecasting strategy for electronic nose performance. *Sens. Actuators B Chem.* **2005**, *106*, 101–113. [[CrossRef](#)]
13. Snopok, B.A. Nonexponential Kinetics of Surface Chemical Reactions (Review). *Theor. Exp. Chem.* **2014**, *50*, 67–95. [[CrossRef](#)]
14. Snopok, B.A.; Snopok, O.B. Information Processing in Chemical Sensing: Unified Evolution Coding by Stretched Exponential. In *Nanostructured Materials for the Detection of CBRN*; Springer: Berlin/Heidelberg, Germany, 2018; pp. 233–244. ISBN 978-94-024-1303-8.
15. Burlachenko, J.; Kruglenko, I.; Manoylov, E.; Kravchenko, S.; Krishchenko, I.; Snopok, B. Virtual sensors for electronic nose devices. In Proceedings of the 2019 IEEE International Symposium on Olfaction and Electronic Nose (ISOEN), Fukuoka, Japan, 26–29 May 2019; pp. 1–3.
16. Snopok, B.A.; Kruglenko, I.V. Multisensor systems for chemical analysis: State-of-the-art in electronic nose technology and new trends in machine olfaction. *Thin Solid Film.* **2002**, *418*, 21–41. [[CrossRef](#)]
17. Burlachenko, Y.V.; Snopok, B.A. Methods of cluster analysis in sensor engineering: Advantages and faults. *Semicond. Phys. Quantum Electron. Optoelectron.* **2011**, *13*, 393–397. [[CrossRef](#)]
18. Filippov, A.P.; Strizhak, P.E.; Serebry, T.G.; Snopok, B.A. Direct identification of volatile organic vapors in complex mixtures: Advanced chemical imaging of analytes by cross-reactive sensor arrays with temporal separation. *Sens. Lett.* **2014**, *12*, 1259–1266. [[CrossRef](#)]
19. Kruglenko, B.A., IV. Snopok Thin-film coating of dibenzotetraazaannulenes for quantitative determination of hydrochloric acid vapor by quartz crystal microbalance method. *Theor. Exp. Chem.* **2018**, *54*, 53. [[CrossRef](#)]
20. Filippov, A.P.; Strizhak, P.E.; Serebrii, T.G.; Tripol'Skii, A.I.; Snopok, B.A.; Khavrus, V.; Ivashchenko, T.S. New coating materials for hydrocarbon discrimination using a multisensor system and gas chromatography. *Theor. Exp. Chem.* **2005**, *41*, 389–394. [[CrossRef](#)]

21. Burlachenko, J.I.; Kruglenko, B.; Snopok, K. Persaud Sample handling for electronic nose technology: State of the art and future trends. *Trends Anal. Chem.* **2016**, *82*, 222–236. [[CrossRef](#)]
22. Reznik, A.M.; Shirshov, Y.M.; Snopok, B.A.; Nowicki, D.W.; Dekhtyarenko, A.K.; Kruglenko, I.V. Associative memories for chemical sensing. In Proceedings of the 9th International Conference on Neural Information Processing, 2002. ICONIP '02, Singapore, 18–22 November 2002; Volume 5, pp. 2630–2634. [[CrossRef](#)]